(1)

CORROSION OF GRAPHITE ALUMINUM METAL MATRIX COMPOSITES

by

M.A. Buonanno, R.M. Latanision, L.H. Hihara and J.F. Chiang

Technical Report No. 3
to
Office of Naval Research
Grant No. N00014-89-J-1588

The H.H. Uhlig Corrosion Laboratory
Department of Materials Science and Engineering
Massachusetts Institute of Technology
Cambridge, Massachusetts 02139

February 1991

SECURITY CLASSIFICATION OF THIS PAGE

REPORT DOCUMENTATION PAGE

Form Approved
OMB No. 0704-0188

1a. REPORT SECURITY CLASSIFICATION Unclassified	1b. RESTRICTIVE MARKINGS
2a. SECURITY CLASSIFICATION AUTHORITY	3. DISTRIBUTION/AVAILABILITY OF REPORT
2b. DECLASSIFICATION/DOWNGRADING SCHEDULE	
4. PERFORMING ORGANIZATION REPORT NUMBER(S)	5. MONITORING ORGANIZATION REPORT NUMBER(S)
6a. NAME OF PERFORMING ORGANIZATION Massachusetts Institute of Technology 6b. OFFICE SYMBOL (If applicable)	7a. NAME OF MONITORING ORGANIZATION Office of Naval Research
6c. ADDRESS (City, State, and ZIP Code) Room 8-202, 77 Massachusetts Avenue Cambridge, MA 02139	7b. ADDRESS (City, State, and ZIP Code) 800 N. Quincy Street Arlington, VA 22217-5000
8a. NAME OF FUNDING/SPONSORING ORGANIZATION Office of Naval Research 8b. OFFICE SYMBOL (If applicable)	9 PROCUREMENT INSTRUMENT IDENTIFICATION NUMBER
8c. ADDRESS (City, State, and ZIP Code) Arlington, VA 22217-5000	10. SOURCE OF FUNDING NUMBERS PROGRAM ELEMENT NO. 89-J-1588 / PROJECT NO. cor5523-02 / TASK NO / WORK UNIT ACCESSION NO

11. TITLE (Include Security Classification)

Corrosion of Graphite Aluminum Metal Matrix Composites

12. PERSONAL AUTHOR(S)
M.A. Buonanno, R.M. Latanision, L.H. Hihara and J.F. Chiang

13a. TYPE OF REPORT	13b. TIME COVERED	14. DATE OF REPORT (Year, Month, Day)	15. PAGE COUNT
Technical Report	FROM 1Mar 90 TO 31Dec 90	February 1991	21

16. SUPPLEMENTARY NOTATION

17. COSATI CODES			18. SUBJECT TERMS (Continue on reverse if necessary and identify by block number)
FIELD	GROUP	SUB-GROUP	Corrosion, Graphite Aluminum, Metal Matrix Composites

19. ABSTRACT (Continue on reverse if necessary and identify by block number)

Several commercial G/Al MMCs have been studied by potentiodynamic polarization in deaerated 0.5 M Na_2SO_4. The results have been compared with those which were predicted by the mixed electrode theory. The results indicate that processing conditions, especially the cooling rate, had a strong influence on the corrosion behavior of the G/Al MMCs.

Large scale G/Al model MMCs were fabricated at MIT in order to study the corrosion behavior of G/Al galvanic couples with the scanning potential microprobe (SPM). Preliminary results indicate that coating graphite with discontinuous alumina did not reduce the corrosion rate of the G/Al galvanic couple. Ion implanting the surface of G/Al model MMCs with zinc, a cathodic inhibitor, did reduce the corrosion rate of the G/Al galvanic couple; however, the protection was incomplete.

20. DISTRIBUTION/AVAILABILITY OF ABSTRACT ☒ UNCLASSIFIED/UNLIMITED ☐ SAME AS RPT ☐ DTIC USERS	21. ABSTRACT SECURITY CLASSIFICATION Unrestricted
22a. NAME OF RESPONSIBLE INDIVIDUAL A.J. Sedriks	22b. TELEPHONE (Include Area Code) (202) 696-4401 / 22c. OFFICE SYMBOL 1131 M

DD Form 1473, JUN 86 Previous editions are obsolete SECURITY CLASSIFICATION OF THIS PAGE

Corrosion of Graphite Aluminum Metal Matrix Composites •

M. A. Buonanno*, R. M. Latanision**, L. H. Hihara†, and J. F. Chiang††
Department of Materials Science and Engineering,
MIT, Cambridge, MA 02139

Abstract

Several commercial G/Al MMCs have been studied by potentiodynamic polarization in deaerated 0.5 M Na_2SO_4. The results have been compared with those which were predicted by the mixed electrode theory. The results indicate that processing conditions, especially the cooling rate, had a strong influence on the corrosion behavior of the G/Al MMCs.
Large scale G/Al model MMCs were fabricated at MIT in order to study the corrosion behavior of G/Al galvanic couples with the scanning potential microprobe (SPM). Preliminary results indicate that coating graphite with discontinuous alumina did not reduce the corrosion rate of the G/Al galvanic couple. Ion implanting the surface of G/Al model MMCs with zinc, a cathodic inhibitor, did reduce the corrosion rate of the G/Al galvanic couple; however, the protection was incomplete.

* Research Assistant, MIT, Cambridge, 02139
** Professor of Materials Science and Engineering, MIT, Cambridge, MA 02139
† Assistant Professor, Univ. of Hawaii at Manoa, Honolulu, HI 96822
†† Professor of Chemistry, College at Oneonta, Oneonta, N.Y. 13820

• Paper presented at the 1990 TMS Fall Meeting, Detroit, Michigan, USA October 7-11, 1990; Environmental Effects on Advanced Materials IV: Aqueous Environments. To be published in conference proceedings.

Introduction

Graphite Aluminum (G/Al) Metal Matrix Composites (MMCs) have been shown to possess many attractive mechanical properties [1-3]. Currently, MMCs are being considered for structural components in aircraft and other applications where superior specific strength and weight savings are important parameters. However, because they are susceptible to galvanic corrosion [4-7] their application has been limited. It has long been known that there is a synergistic corrosion effect due to the galvanic electrical contact at the fiber-matrix interface in MMCs. Therefore, MMCs are usually fabricated with a protective coating (e.g., covering exposed areas with aluminum foil) to avoid such galvanic problems; however, it has been shown that such coatings can be compromised during fabrication, structural assembly, usage or by chemical environment [8-10]. More recently, chemical passivation of protective coatings has been shown to increase their corrosion resistance [11]. Although these techniques improve the corrosion resistance of MMCs, it would also be desirable to improve the corrosion characteristics of the inherent composite fiber/matrix couple in order to ensure the integrity of the components, in case the protective coating should be compromised during service. It is also necessary that remedies to reduce corrosion (e.g., insulating coatings, matrix modification, processing conditions, etc.) do not degrade the mechanical properties of the MMCs in such a way as to preclude their use. This study is aimed directly at understanding what can be done to reduce the corrosion that occurs to the inherent G/Al MMC system.

Mixed-Electrode Theory

The corrosion of G/Al MMCs has been studied extensively [11]. These results have shown that the galvanic effect in MMCs can be accurately modelled with the mixed-potential theory. Commercial MMCs studied were produced by a process known as diffusion bonding. This process left behind trace microstructural chlorides, which increased the corrosion rate of the composite significantly [12]. As will be shown, the anodic potentiodynamic behavior of the diffusion bonded commercial G/Al MMC deviated significantly from that which was predicted by the mixed electrode theory. This study compares the anodic potentiodynamic behavior of several new commercial G/Al MMCs, produced without microstructural chlorides, in deaerated 0.5M Na_2SO_4 solution.

Corrosion Inhibition Schemes

While the galvanic corrosion behavior of G/Al MMCs has been well established, it was decided that the problem of controlling corrosion should be addressed. Hihara and Latanision considered cathodic protection, electronic insulation of fibers and ion implantation of graphite with cathodic inhibitors as corrosion control schemes for G/Al MMCs [11]. It was concluded that cathodic protection of G/Al MMCs resulted in overprotection [13]. Overprotection resulted from a local increase in pH near cathodic sites during polarization. It was pointed out that cathodic protection required careful control of the cathodic potential in order to avoid alkanization of cathodic sites, thereby rendering this form of corrosion control unreliable. Therefore, this study will address, electronic insulation of fibers, and ion implantation of graphite with zinc, as methods to reduce the corrosion rate of the G/Al MMC system.

Experimental

Potentiodynamic Tests

Polarization of commercial MMCs was accomplished with a model 273 EG&G Princeton Applied Research (PAR) potentiostat. The ASTM G-5 standard for polarization of 430 stainless steel in deaerated 1N H_2SO_4 was reproduced to determine the apparatus reliability [14]. The results were reproducible and gave the accepted current potential relationship according to the ASTM G-5 standard. All polarization tests conducted on G/Al MMCs were carried out in H_2 purged 0.5M Na_2SO_4 (pH = 7) at 30°C. The electrodes were allowed to stabilize at their corrosion potentials, E_{corr}, and were subsequently polarized at a rate of 0.1 mv/s. At least three individual tests were performed for each commercial MMC.

Materials

Four commercial continuous fiber G/Al MMCs were studied. Their characteristics are given in Table 1. The specimen received by DWA Composite Specialties, Inc., Chatsworth, CA. was produced by a diffusion bonding process that was shown to leave behind residual chlorides between fiber tows which have been diffusion-bonded; these results have been documented elsewhere [12]. All other commercial MMCs were produced by a pressure infiltration process. The G/Al MMC made by MIT was cooled with a known cooling rate of 50°C/min [15]. The cooling rate of the G/Al MMCs made by Aluminium Ranshofen is known to have been less than 50°C/min.

Table 1. Commercial MMCs Studied

Producer	Matrix Composition	Fiber Mod. Msi	% Fiber	Fabrication Technique
DWA Composite Specialties	6061 Al T-6	100	50	Diffusion Bonded Tows
Aluminium Ranshofen	6061 Al T-6	56.8	64	Infiltration
Aluminium Ranshofen	"Type 2000 Al"	56.8	62	Infiltration
MIT	1100 Al	58	55	Infiltration

*All composites were continuous fiber MMCs
Note T-6 heat treatment:
1. Solutionize at 527°C for 1 hr. 2. Water quench. 3. Age at 177°C for 8 hrs.

Results and Discussion

The mixed electrode theory, which states that the absolute value of the total sum of cathodic current must equal the total sum of the anodic current, was used to predict the anodic behavior for G/6061-T6 Al couple with a fiber volume fraction of 50%, Fig. 1. Mathematically this is achieved be adding half the anodic current density values of graphite fiber to half of the anodic current density values of 6061-T6 Al, attained from separate anodic polarization experiments performed on graphite fibers and 6061-T6 Al in deaerated 0.5M Na_2SO_4 [11]. The polarization behavior indicates that a passivation region should be attainable from -1000 to 300 mV_{sce}. Above 300 mV_{sce} the anodic behavior of the graphite begins to dominate the polarization behavior, causing a subsequent increase in the corrosion current density. In Fig. 2 the results of anodic polarization of the four commercial G/Al MMCs studied have been superimposed for comparison. The predicted anodic behavior for the G/6061-T6 Al MMC has been corrected for a fiber volume fraction of 55%. In comparing these MMCs it is apparent that the MMC that had residual microstructural chlorides, the DWA diffusion bonded material, had the poorest corrosion resistance. The two commercial MMCs received from Aluminium Ranshofen, although slightly different in composition, when plotted with error bars (not shown here) were within experimental error of each other; therefore, it could not be concluded that the MMC that contained copper (i.e., G/2000 Al) behaved significantly different from the G/6061-T6 Al MMC. The G/1100 Al MMC produced at MIT, showed significant corrosion resistance when compared to all other commercial MMCs studied by anodic polarization. Of all the commercial MMCs tested, the anodic polarization behavior of G/1100 Al MMC was the most similar to that predicted by the mixed electrode model. This MMC was cooled at 50°C/min. The cooling rate of the MMCs received from Aluminium Ranshofen was less than this; however, the specific cooling rate is proprietary and can not be disclosed. There are three possibilities for the improved behavior of the MIT G/1100 Al MMC: 1) the alumina film formed on 1100 pure Al was more resistant to breakdown than for alloyed aluminium, 2) the 1100 pure Al matrix has less impurities, changing the chemistry of the reactions at the G/Al interface during infiltration, and 3) the higher cooling rate of the MMC produced at MIT suppressed the amount of Al_4C_3 formed at

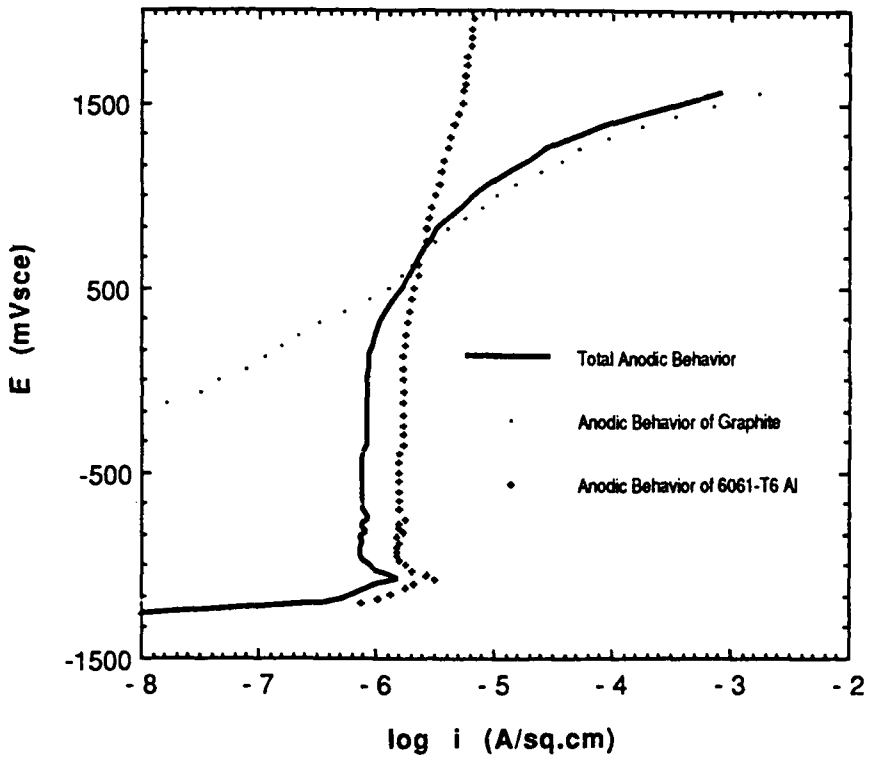

Fig. 1. The predicted G/6061-T6 Al MMC (fiber volume fraction = 50%) anodic behavior in deaerated 0.5 M Na_2SO_4.
[Ref.: L. H. Hihara, "Corrosion of Aluminum-Matrix Composites," Ph.D. thesis, MIT, 1989, p.152]

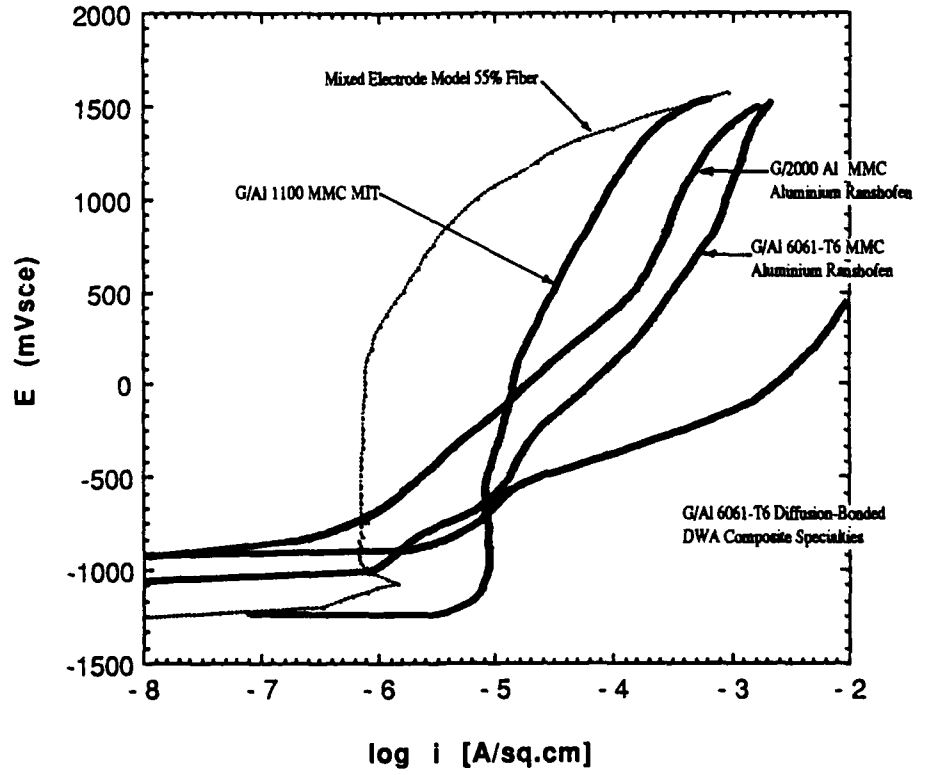

Fig. 2. The anodic potentiodynamic behavior in deaerated 0.5 M Na_2SO_4 of several commercial G/Al MMCs compared to that predicted by the mixed electrode theory for a G/6061-T6 Al MMC (fiber volume fraction = 55%).

the G/Al interface as compared to that produced by Aluminium Ranshofen. In deaerated 0.5M Na_2SO_4, both ultra pure Al (99.999) and 6061-T6 Al remain passive during anodic polarization [11]. This similar anodic polarization behavior suggested that alloying elements of 6061-T6 Al had no significant effect on the dissolution characteristics of the passive alumina film. Therefore, it is probable that the second and third possibility, change in interfacial reaction chemistry and increased importance of the cooling rate during processing were more important parameters. Furthermore, in comparing the G/2000 Al MMC specimen from Aluminium Ranshofen that contained copper, the results indicate that the anodic corrosion characteristics for this MMC did not deviate significantly from the Aluminium Ranshofen G/6061-T6 Al made without copper. Copper is known to increase the corrosion susceptibility of Al alloys, since O_2-reduction occurs at a much higher rate on relatively cathodic Cu than on Al. It is therefore concluded that the impurity level was not as important a parameter as the cooling rate for the corrosion resistance of the G/Al MMCs studied.

G/Al Model Metal Matrix Composites

Fabrication of Model Metal Matrix Composites

Large scale G/Al model MMCs were made at MIT. These interfaces were then examined with the scanning potential microprobe (SPM) at the Marine Biology Laboratory (MBL), Woods Hole, MA, to elicit new information concerning the chemical stability of the interface *in-situ*. The SPM will be discussed later on.

Graphite rod, 0.762 mm (700 μm) in diameter and 30.5 cm in length, was supplied by Micro Mechanics Inc, Ipswitch, MA. The pitch-base graphite rod was completely graphitized. To produce G/Al model MMCs, a small furnace was made at MIT, Fig. 3. 99.99% pure aluminum was melted at 680°C in a specially coated quartz tube. The quartz tube was coated beforehand with a diffusion barrier (Formkote T50 ™, EM Corporation, Indiana) in order to prevent silicon from entering the melt. A Teflon cap was inserted after the aluminum had reached 680°C. The Teflon cap was machined to fit and hold the graphite rod in place during solidification. Although this technique was not performed under hydrostatic pressure, it did facilitate water quenching. This minimized the amount of contact time between the aluminum and graphite. Secondary electron SEM observation, Fig. 4, of prepared samples showed that the G/Al interface contained no large aluminum carbide (Al_4C_3) platelets. After a thorough investigation by SEM, no submicron platelets of Al_4C_3 were observed. All specimens were observed by optical light microscope at 1000X; none of the specimens produced showed Al_4C_3 formation.

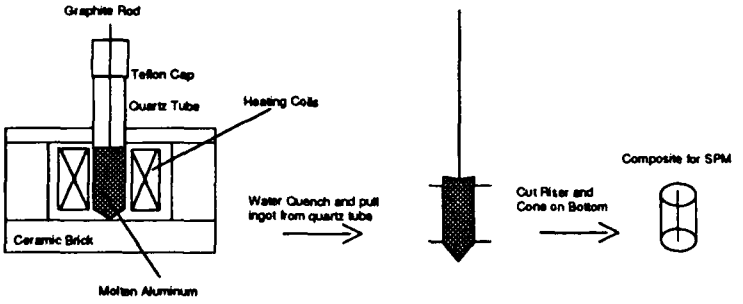

Fig. 3. Schematic for the fabrication of G/Al model MMCs prepared at MIT.

Two different sized quartz tubes were used, having 11 mm and 16 mm inner diameters. This was done so that comparisons could be made from the SPM results as a function of anodic surface area. Uncoated specimens were metallurgically polished to 0.3 μm with gamma alumina powder in pure water (18 MΩ cm).

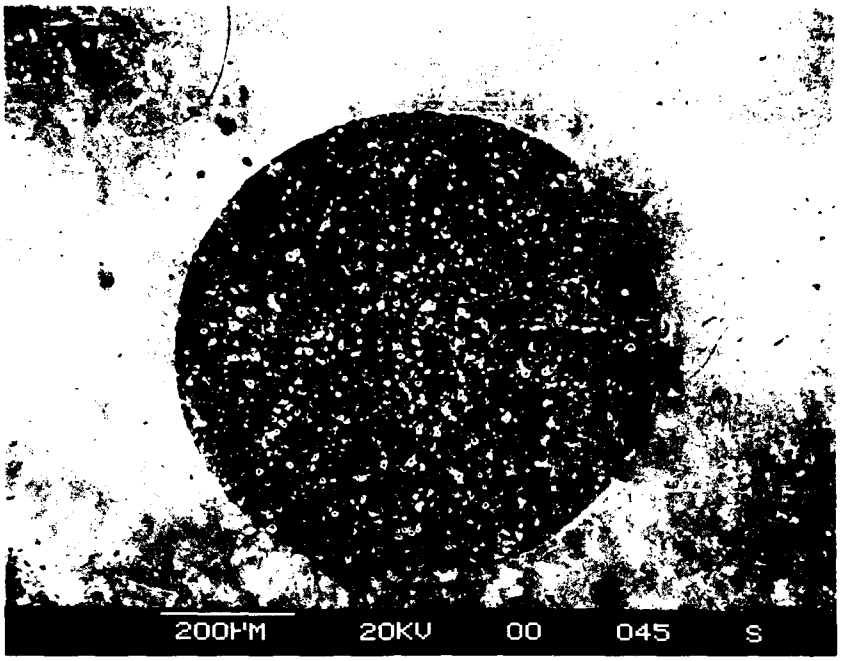

Fig. 4a. Secondary electron SEM image of graphite rod in 99.99% Al (i.e., G/Al model MMC). Note the absence of any crevices.

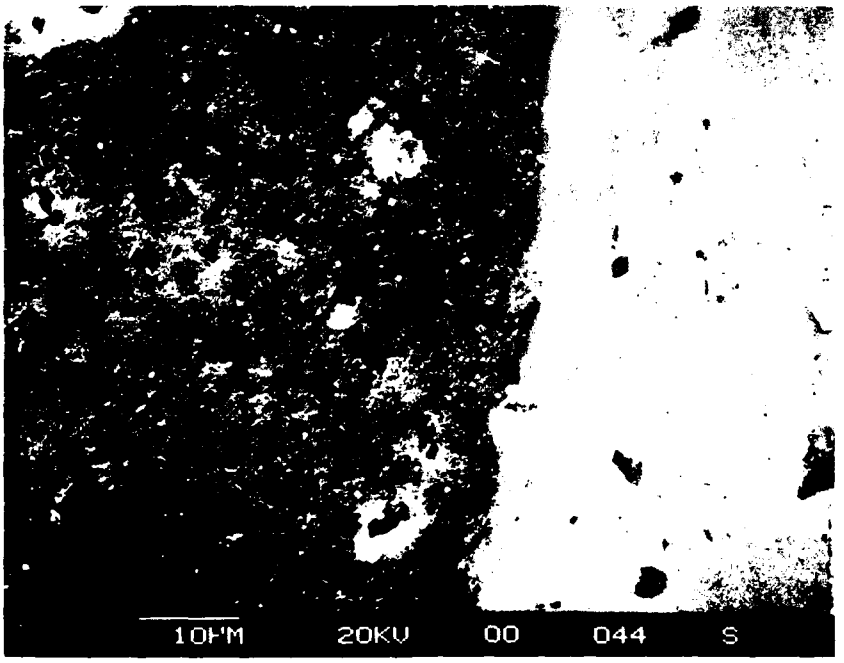

Fig. 4b. Higher magnification of representative region of G/Al model MMC interface. Good interfacial contact was achieved.

Alumina Coating of Graphite Rod

In order to coat the rod with alumina (Al_2O_3), the alkoxide route was adopted. This technique has been reviewed by Katzman for silica formation in a toluene base solvent [16, 17]. The technique was successful in producing fine silica films, and it was reported to also work well in forming fine alumina films [18]. A solution of toluene based 8 vol% aluminum isopropoxide ($Al(OC_3H_7)_3$) was ultrasonically mixed for thirty minutes. The graphite rod was baked overnight at 200°C in order to remove any moisture and contamination, and then placed in solution and ultrasonically coated for thirty seconds and removed. In order to hydrolyze the coating, the rod was placed above a boiling mixture of pure water (18 MΩ cm) for thirty seconds. Finally, the rod was placed in a tube furnace containing an argon atmosphere at 500°C for about one minute in order to vaporize any excess solvent or water and to pyrolyze any unhydrolyzed organometallic compounds. The entire procedure was then repeated in order to ensure that the coating completely covered the rod. The rod was viewed by SEM, Fig. 5. The coating was rough and porous in nature; however, there were no apparent bare spots; the rod seemed completely coated. Energy dispersive analysis of X-rays (EDAX) revealed only aluminum, indicating that the film was most probably alumina. Auger electron spectroscopy (AES) was also used to determine that the coating was Al_2O_3. Known spectra for Al_2O_3 were compared to that obtained from this coating; they were of the same shape and energy. AES was also used to estimate the thickness of the coating. A 1000Å tantalum oxide/ tantalum sample was argon ion sputtered until the 1000Å oxide was removed. Under the same conditions the alumina coated graphite rod was sputtered until the alumina was removed. The rate of oxide removal was assumed to be the same for the tantalum oxide and alumina. From these results the alumina film was on the order of 4000Å thick. Subsequently, this rod was used for the production of G/Al model MMCs, as outlined in the previous section. All G/Al model MMCs, except those ion implanted with zinc were metallurgically polished to 0.3 μm with gamma alumina powder in pure water (18 MΩ cm). They were re-polished with 0.25 μm diamond paste mixed with pure water and thoroughly rinsed prior to SPM scans at MBL.

Zinc Ion Implantation of Model Metal Matrix Composites

Uniform ion implantation along the circumferential area of the cylindrical graphite rods was not feasible, therefore, it was decided to implant the surface of the G/Al model MMC, Fig. 6. Ion implantation with Zn^{2+} cations would only be achievable for implantation depths on the order of 1000Å, and therefore the specimens could not be polished after the implantation or the implanted layers would be removed. The ion implantation beam energies and doses given to two uncoated G/Al model MMCs of 11 mm and 16 mm diameter appear in Table 2.

Table 2. Zinc Ion Implantation Data

Beam Energy (KeV)	Concentration (atoms/cm^2)
75	1.2×10^{14}
100	1.2×10^{14}
125	1.2×10^{14}
150	1.2×10^{14}
175	1.2×10^{14}

The various beam energies were employed so that a more even concentration level of zinc would be attained. It is expected that the depth of implantation was on the order of 1000Å.

The idea behind ion implanting with zinc is to place zinc atoms in the graphite, so that they can become solvated as zinc cations when the composite comes in contact with solution. Thereafter, the zinc cations could migrate to the G/Al interface and exposed graphite surfaces to form $Zn(OH)_2$. This corrosion product could then limit the galvanic corrosion process between the graphite and aluminum by reducing the cathodic O_2-reduction reaction which occurs on graphite. Thus zinc is a cathodic inhibitor in this process. Addition of as little as 10 ppm $ZnCl_2$, a cathodic inhibitor, to aerated 3.15 wt% NaCl solutions, has shown that it is possible to decrease the corrosion rate of G/Al galvanic couples by a factor of 10-100 [11].

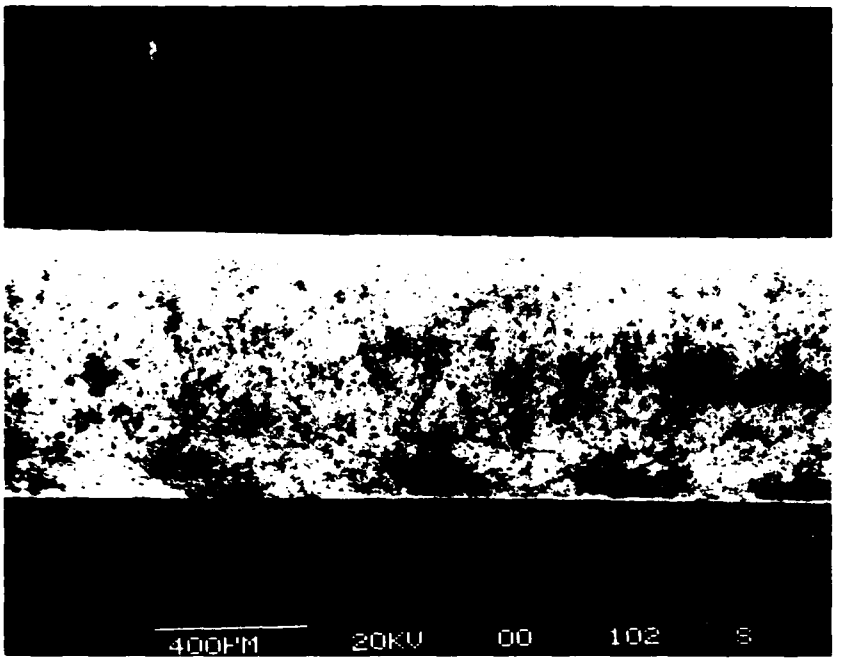

Fig. 5. Secondary electron SEM image of alumina coated graphite rod. The rod is completely coated; however, the coating appears porous.

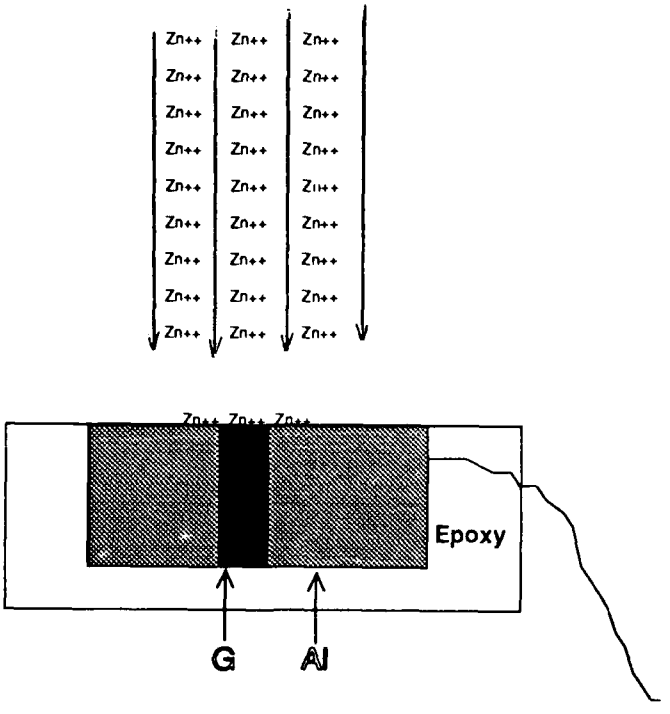

Fig. 6 Schematic of zinc ion implantation geometry accomplished on the surface of the G/Al model MMCs.

The Scanning Potential Microprobe/Scanning Vibrating Electrode Technique

Large scale model composites were investigated using the scanning vibration electrode technique (SVET). Scheffey and Isaacs have extensively reviewed this technique elsewhere [19-23]; details of the probe electronics used at MBL are also available [18]; only a brief overview will be given to acquaint the reader.

The SVET enables the researcher to measure ionic currents associated with corrosion microcells with spatial and current resolutions on the order of 15 to 20 μm and 5 nA/cm^2, respectively [24]. The SVET consists of vibrating a very fine electrode at a fixed frequency over the surface of a specimen immersed in an electrolyte. The electrode measures the difference in the electric field potential near the surface of the specimen compared to a point further away from the surface. The probe is vibrated vertically and horizontally by a piezoelectric vibrating reed made of lead zirconium titanate. By applying two different sinusoidal voltages to three coupled bimorphs, the probe tips deflect approximately 20 μm peak to peak in the vertical and horizontal direction. The voltage at the two extremes of vibration is measured, relative to a distant Pt reference electrode, and used to calculate the current density component of the medium at the center point of vibration, and tangential to the direction of vibration according to [24].

$$i\ (A/cm^2) = \sigma\ (\Omega cm)^{-1}\ \Delta V(volts)/\Delta r\ (cm) \qquad (1)$$

where i is the current density component parallel to probe vibration, ΔV is the voltage difference between the extremes of vibration, Δr is the vibration stroke, and σ is the conductivity of the solution. Therefore, a current density of 50 μA/cm^2 would correspond to a voltage difference of 100 μV, which is a very small potential difference. Thus the SVET has a greater sensitivity than techniques which do not use a vibrating probe (i.e., stationary probes). The high resistivity of this solution allowed for excellent spatial resolution. The measured resistivity of this solution was 920 Ω cm. The probe employed had a diameter of 15 μm. The relationship for rms current noise is

$$i\ (A/cm^2) = 3\times10^{-11}/d\ (cm)^{3/2}\rho\ (\Omega cm)^{1/2} \qquad (2)$$

where d is the electrode tip diameter, and ρ is the electrolyte resistivity [20]. Thus, the minimum

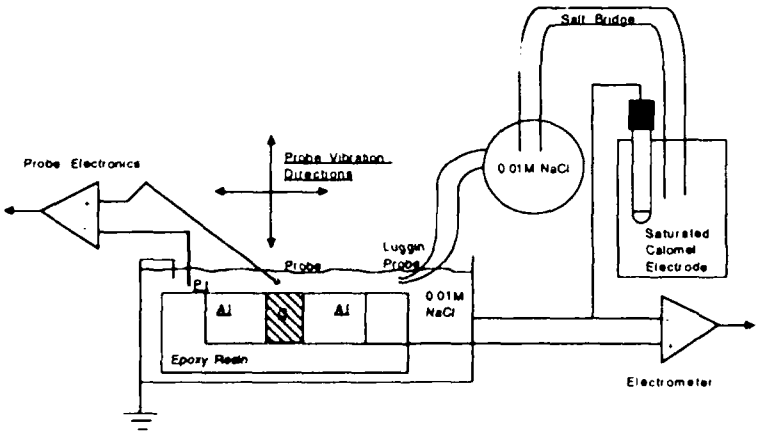

Fig. 7 Schematic of SPM assembly used to study G/Al model MMCs at the Marine Biological Laboratory (MBL), Woods Hole, MA.

rms current noise for each measurement of each component of the field vector, assuming that current noise was due only to the thermal noise of resistance in the electrolyte between the electrode surface and distant ground, was ±0.02μA/cm^2. Data was acquired for ten seconds for each scan point measured. The probe measurements were taken at 500 μm above the surface in order to subtract the background current from the desired surface measurements, which were

taken from a height of approximately 50 μm above the surface of the sample. Current density vectors measured by the probe were superimposed upon a video image of the investigated specimen. The current density vectors were graphically represented as arrows starting at the position of the observation and with length and direction representing the field measurement. The digitized images of the specimens were stored on computer disk, and field measurements were stored separately; selected measurements could be re-plotted with arbitrary scale on the corresponding sample.

In this study the corrosion potential, E_{corr}, of the G/Al model MMCS with reference to the saturated calomel electrode was also monitored, Fig. 7. The results were monitored with a chart recorder for the period of time that the sample was tested by the SVET, approximately 20 minutes. All tests performed were conducted in air. Each specimen was scanned with probe steps of about 45 μm for each measurement.

Results and Discussion

Model G/Al MMCs

Video images were photographed of G/Al model MMC samples at the beginning of the corrosion study, Fig 8. Fig. 9 reveals the same samples after having been left in 0.01M NaCl for 48 hours. The superimposed vectors in Figs. 8 and 9 give the current density vectors measured by the SVET technique. The probe was vibrated in two directions; normal to the surface, the z direction; and in the x direction. A superimposed vector in the figure pointing in the negative y direction represents a net cathodic ionic current, which flows in the negative z direction. While a positive y component of a current density vector indicates a net anodic current coming out (positive z direction) of the specimen towards the viewer. The x component of the superimposed current density vector gives the actual direction of the net ionic current in the x direction. The movement of specific ionic species in the solution is impossible to determine from the SVET, which in this case only monitors the net ionic current; however, one should think of the movement of ionic species as an integral part of what is being measured by the SVET. In this case, such species as Al^{+3}, OH^-, H^+ and $Al(OH)^{+2}$ are flowing from the surface through the solution. It should be pointed out that only the y component of the current density vector was used in determining the cathodic and anodic nature of the measured current in Fig. 10.

It was arbitrarily decided to consider the G/Al interface as a reference point; cathodic current densities were measured at a point 90 μm from the interface over the embedded graphite rod while, anodic current densities were measured at a distance of approximately 180 μm from the interface over the aluminum. In this way, current density values could be compared over a period of time. Fig. 10, reveals the results for the four samples tested. The open circuit potential of the uncoated sample was the most electropositive, Fig. 10a. The value was approximately -0.55 V_{sce}; the very high value was due to the presence of oxygen; the tests were performed in air. As time elapsed, the value for E_{corr} moved to more active (negative) values; presumably, this was due to the breakdown of the protective oxide film covering the aluminum.

The corrosion potential of the alumina coated specimen followed a similar trend, Fig. 10a, indicating that the coating did not resist the flow of electrons at the G/Al interface. In fact, the alumina coated specimen corroded the quickest of all samples tested. The sample formed a crevice after a period of 24 hours.

The cathodic current densities as a function of time, Fig. 10b, for the uncoated and alumina coated samples decreased after 24 hours. Thereafter, the cathodic current densities of these specimens increased with time as expected. The initial decrease in cathodic current densities at this time is not understood, and more testing must be performed.

Of the two zinc ion implanted specimens tested, only the specimen which had an 11 mm diameter showed a consistent decrease in corrosion current densities after 48 hours, Fig. 10b and 10c. Both the cathodic and anodic current densities decreased significantly after a period of 24 hours. For the 11 mm diameter zinc ion implanted specimen, the cathodic current density decreased by a factor of 12 after 24 hours, Fig. 10b, while after 48 hours the cathodic current density had dropped by a factor of 20 from the initial cathodic current density. The 16 mm diameter zinc ion

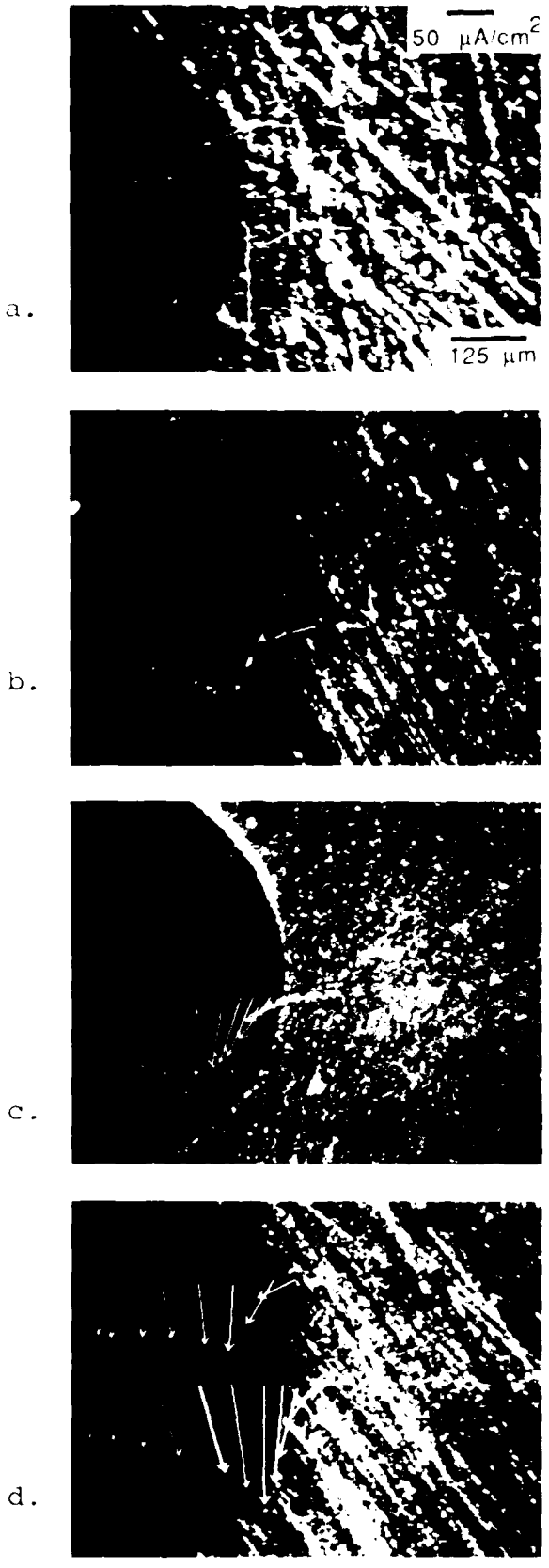

Fig. 8 SPM video images taken of 16 mm diameter G/Al model MMCs in 0.01 M NaCl at initiation of test, time = 0: (a) uncoated graphite (b) alumina coated graphite (c) zinc ion implanted, and (d) zinc ion implanted but with 11 mm diameter.

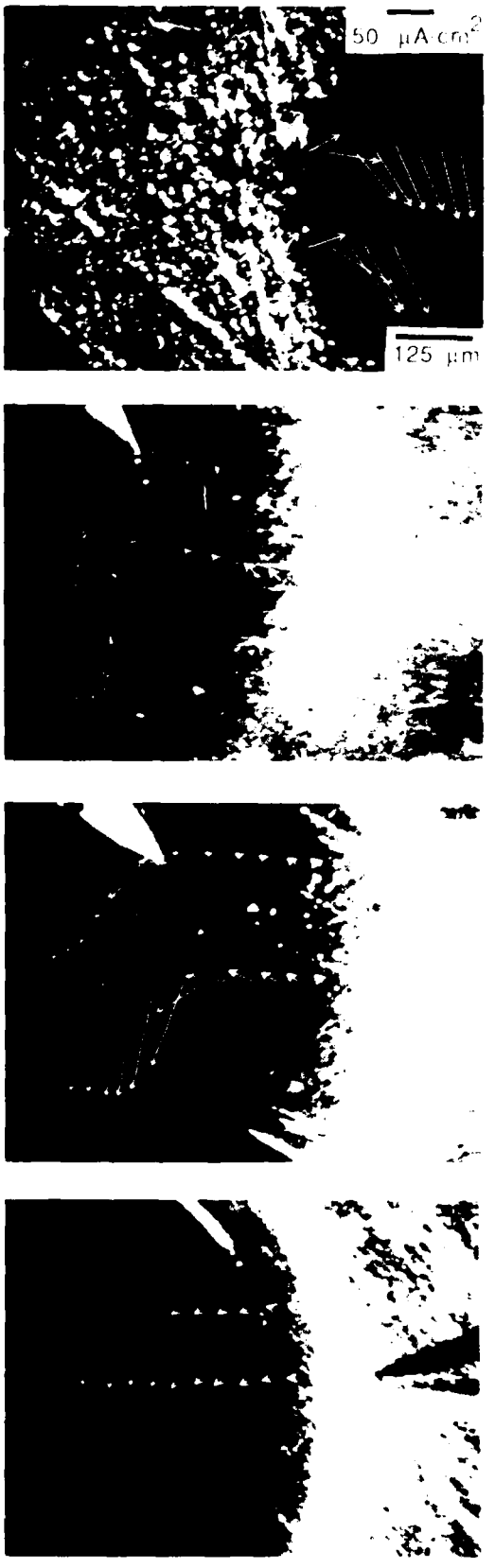

Fig. 9 SPM video images taken of 16 mm diameter G/Al model MMCs in 0.01 M NaCl at, time = 48 hours: (a) uncoated graphite (b) alumina coated graphite (c) zinc ion implanted, and (d) zinc ion implanted but with 11 mm diameter.

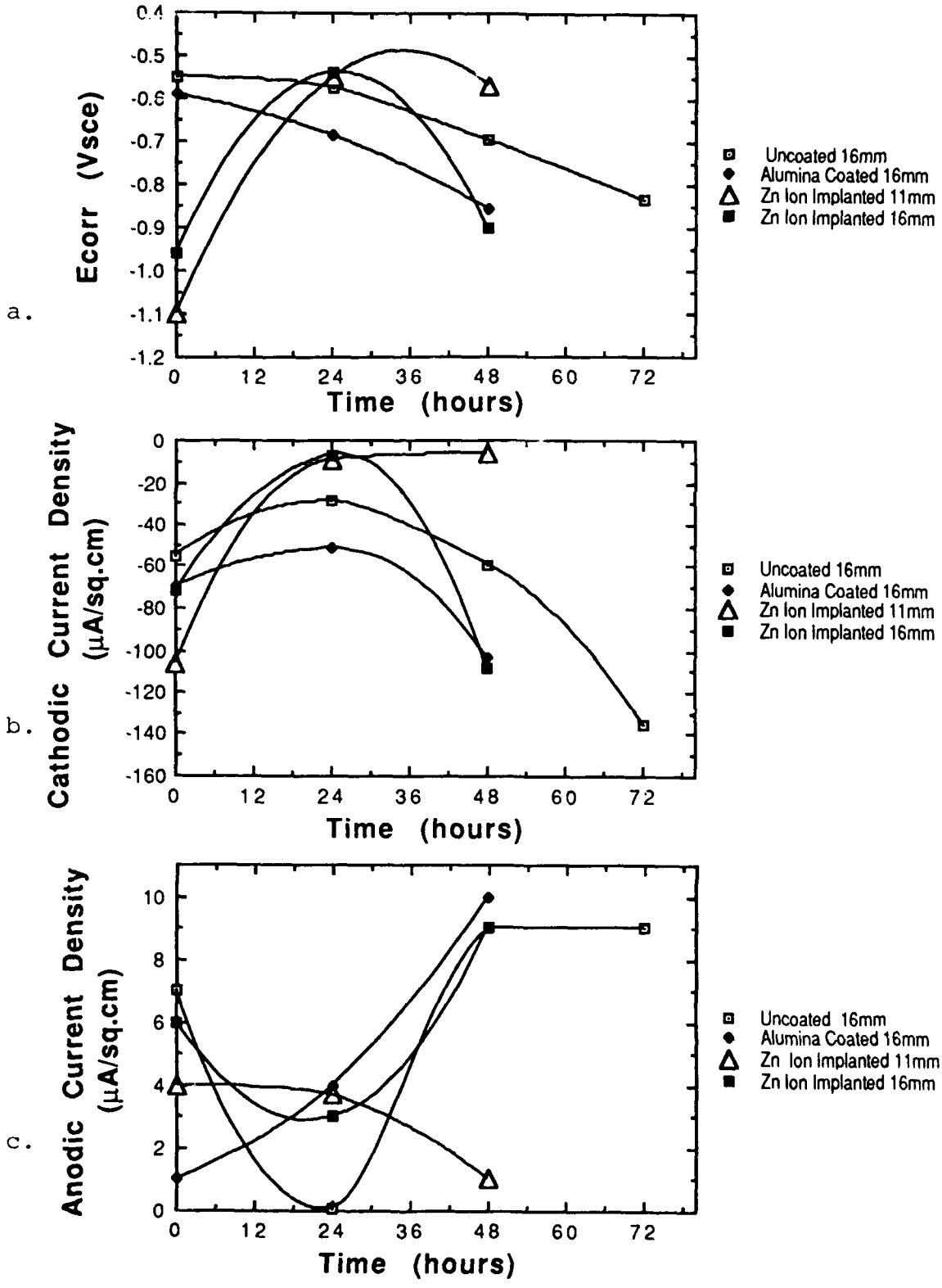

Fig. 10 Graphic representation of SVET test results: (a) the monitored open circuit potential measured against the saturated calomel electrode vs. time in solution, (b) cathodic current density measured at 90 μm from the G/Al interface, over the graphite rod, and (c) the anodic current density measured at 180 μm from the G/Al interface, over the aluminium matrix.

implanted specimen showed a similar decrease in corrosion current densities after 24 hours, Fig. 10b and 10c; however, after 48 hours both the anodic and cathodic current density values began to increase and a crevice formed at the G/Al interface. One possible explanation for the different behavior is that the anodic area was greater for the 16 mm zinc ion implanted specimen and hence the cathodic current density over the graphite rod was greater. After 24 hours in solution the cathodic current density was greater on the 16 mm zinc ion implanted specimen than that on the 11 mm zinc ion implanted specimen. As zinc became solvated, forming zinc cations, these cations formed $Zn(OH)_2$, covering the graphite and hence, the corrosion current densities decreased. Apparently, the protection was not complete for the 16 mm zinc ion implanted specimen after 48 hours. The ion dosage given, 1.2×10^{14} atoms/cm^2, is a low implanting dosage. It is apparent that higher dosages must be studied to ascertain the level of protection that may be achieved. In near neutral solutions, such as 0.01M NaCl, O_2-reduction leads to localized alkalinity by the reaction,

$$O_2 + 2H_2O + 4e^- \rightarrow 4(OH)^- \qquad (3)$$

which increases the alkalinity by producing OH^-. Since protection was not complete, O_2-reduction occurred, and the local pH of the graphite surface must have become increasingly alkaline for the 16 mm zinc ion implanted specimen. Fig. 11 is the Pourbaix potentential-pH equilibrium diagram. As can be seen $Zn(OH)_2$ will break down as the alkalinity of the solution becomes greater, shifting to the right of the diagram. This local increase in alkalinity leads to the the break down of the protective $Zn(OH)_2$. Had the 11 mm zinc ion implanted specimen been left in solution longer, it may well have begun to corrode at higher corrosion rates as did the 16 mm diameter zinc ion implanted specimen.

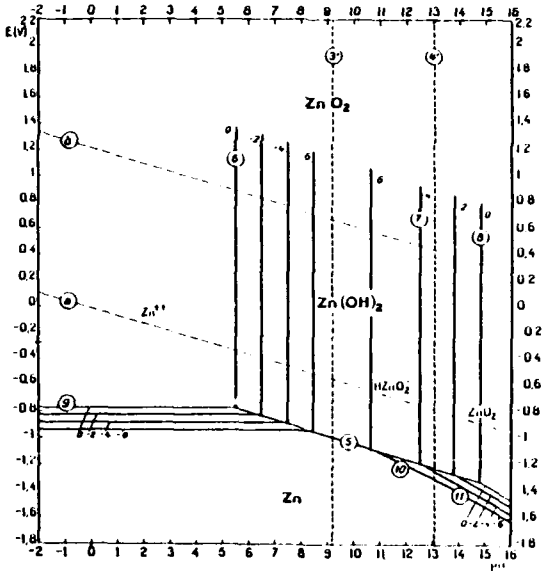

Fig. 11 The pH-potential equilibrium Pourbaix diagram for the system zinc-water, at 25°C. [Ref.: M. Pourbaix, Atlas of Electrochemical Equilibria in Aqueous Solutions, Sec. Eng. Ed., Pergamon Press Ltd., 1974, p. 409]

Conclusions

Potentiodynamic Testing of Commercial G/Al MMCs

1. The commercial G/Al MMC studied that contained microstructural chlorides had the poorest corrosion resistance in deaerated 0.5 M Na_2SO_4. Microstructural chlorides should be avoided during fabrication.

2. All commercial G/Al MMCs studied that contained no microstructural chlorides showed improved corrosion resistance, more closely resembling the polarization behavior predicted by the mixed electrode theory.

3. Anodic potentiodynamic testing of commercial G/Al MMCs indicates that the processing parameters, especially the rate of cooling during fabrication, strongly influenced the corrosion behavior of the commercial G/Al MMCs studied.

G/Al Model MMCs

4. Porous alumina coated graphite did not reduce the flow of electrons across the G/Al interface.

5. Zinc ion implantation on the surface of G/Al model MMCs resulted in a significant decrease in corrosion current densities, and hence corrosion; however, after a period of time this protection broke down for the specimen which had the larger anodic surface area, indicating that for the ion implantation dose given, protection was incomplete.

6. The SPM is a valuable tool for studying the corrosion behavior of MMCs.

Acknowledgments

We are grateful to the office of Naval Research for its support (Grant N00014-89-J-1588) and to Dr. A.J. Sedricks for his interest and encouragement. We wish to acknowledge as well: Dr. J. Cornie, Dr. P. Nagarkar and Dr. M. Kloppers of MIT for many helpful discussions; Dr. H. Katzman of the Aerospace Corp. for coatings; Dr. H. Isaacs for his advice; Dr. P. Degischer and Mr. H. Kaufmann of Aluminum Ranshofen, Austria; Dr. W Harrigan, Jr., of DWA Composite Specialties Inc.; and finally, MBL and Mr. Alan Shipely without whom many of these experiments would not have been possible.

References

1. M.A. Meyers and K.K. Chawla, Mechanical Metallurgy Principles and Applications, (Englewood Cliffs, N.J.: Prentice-Hall, Inc., 1984), 438-466.

2. A. Mortensen, J.A. Cornie and M.C. Flemings, "Solidification Processing of Metal-Matrix Composites," Journal of Metals, (F) (1988), 12-19.

3. M. Taya and R.J. Arsenault, Metal Matrix Composites Thermomechanical Behavior (Elmsford, N.Y.: Pergamon Press, 1989), 5-8.

4. J.E. Hack and M.F. Amateau, eds., Mechanical Behavior of MMCs (Warendale, P.A.: Metallurgical Soc. of AIME, 1983), 335-352.

5. D.M. Aylor, R.J. Ferrara, and R.M. Kain, "Marine Corrosion Behavior and Protection Methods for Graphite/Aluminum Metal Matrix Composites," Corrosion 83 (Paper presented at the International Corrosion Forum sponsored by the NACE, Anahelm, California, 18-22 April 1983), 68/1-68/13.

6. W.F. Czyrklis, "Corrosion Evaluation of Graphite-Aluminum and Graphite-Magnesium Metal Matrix Composites," Corrosion 85 (Paper presented at the International Corrosion Forum, Boston, Massachusetts, 25-29 March 1985), 196/1-196/23.

7. M. Saxena et al., "Corrosion Characteristics of Cast Aluminum Alloy-3 wt% Graphite Particulate Composites in Different Environments," Corrosion Science, 27(3)(1987), 249-256.

8. J.H. Payer and P.G. Sullivan, "Corrosion Protection Methods for Graphite Fiber Reinforced Aluminum Alloys," Bicentennial of Materials (Paper presented at the 8th

National Sampe Technical Conference, Seattle, Washington, 12-14 October 1976), Vol. 8, 343-352.

9. D.M. Aylor, R.J. Ferrara, and R.M. Kain, "Marine Corrosion and Protection for Graphite/Aluminum Metal Matrix Composites," Materials Performance, 23(7)(1984), 32-38.

10. F. Mansfeld et al., "Corrosion Protection of Al Alloys and Al-Based Metal Matrix Composites by Chemical Passivation,"Corrosion 88 (Paper presented at the International Corrosion Forum sponsored by the NACE, St. Louis, Missouri, 21-25 March 1988) 380/1-380/19.

11. L.H. H[illegible]ara, "Corrosion of Aluminum-Matrix Composites" (Ph.D. thesis, MIT, 1989).

12. L.H. Hihara and R.M. Latanision, "Residual Microstructural Chloride in Graphite-Aluminum Metal Matrix Composites," Materials Science and Engineering, A126 (1990), 231-234.

13. L.H. Hihara and R.M. Latanision, "Cathodic Overprotection of SiC/6061-T6 and G/6061-T6 Aluminum Alloy Metal Matrix Composites," Scripta Metallurgica, 22 (1988) 413-418.

14. R. Lukens et al., eds., Annual Book of ASTM Standards, part 10 (Philadelphia, PA: American Society for Testing and Materials, 1980), 816-826.

15. B.E. Kowing, "The Production of Graphite Fiber Reinforced Aluminum Plates Through the Pressure Infiltration and Casting Process" (B.S. thesis, MIT, 1990) 29.

16. H.A. Katzman, "Fibre Coatings for the Graphite-Reinforced Magnesium Composites," Journal of Materials Science, 22 (1987), 144-148.

17. H.A. Katzman, "Fiber Coatings for Composite Fabrication," Materials & Manufacturing Processes, 5(1) (1990), 1-15.

18. H.A. Katzman, private communication with author, The Aerospace Corporation, El Segundo, CA 90245, July 1990.

19. C. Scheffey, "Electric Fields and the Vibrating Probe for the Uninitiated", Ionic Currents in Development, Proceedings of a Satellite Meeting to the 10th International Congress of the International Society of Developmental Biologists, University of California, Los Angeles, California, August 2-4, 1985, (New York: Alan R. Liss, Inc., 1986), xxv-xxxvii.

20. C. Scheffey, "Two Approaches to Construction of Vibrating Probes for Electrical Current Measurement in Solution", Rev. Sci. Instrum, 59(5)1988, 787-792.

21. H.S. Isaacs, "Applications of Current Measurement Over Corroding Metallic Surfaces," Ionic Currents in Development, Proceedings of a Satellite Meeting to the 10th International Congress of the International Society of Developmental Biologists, University of California, Los Angeles, California, August 2-4, 1985, (New York, N. Y.: Alan R. Liss, Inc., 1986), 37-44.

22. H.S. Isaacs, "The Effect of Height on the Current Distribution Measured with a Vibrating Electrode Probe" (Report BNL-43218, U.S. Government, May 1990).

23. H.S. Isaacs, "The Measurement of the Galvanic Corrosion of Soldered Copper Using the Scanning Vibrating Electrode Technique," Corrosion Science, 28(6)(1988), 547-558.

24. C.R. Crowe, "Localized Corrosion Currents from Graphite/ Aluminum and Welded SiC/Al Metal Matrix Composites," (NRL Memorandum Report 5415, Naval Research Laboratory, Feb. 1985).